Since January 2020 Elsevier has created a COVID-19 resource centre with free information in English and Mandarin on the novel coronavirus COVID-19. The COVID-19 resource centre is hosted on Elsevier Connect, the company's public news and information website.

Gene 566 (2015) 47–53

Contents lists available at ScienceDirect

Gene

journal homepage: www.elsevier.com/locate/gene

Research paper

The hepatitis E virus ORF1 'X-domain' residues form a putative macrodomain protein/Appr-1″-pase catalytic-site, critical for viral RNA replication

Mohammad Khalid Parvez *

Department of Pharmacognosy, King Saud University College of Pharmacy, PO Box-2457, Riyadh 11451, Saudi Arabia

ARTICLE INFO

Article history:
Received 26 February 2015
Received in revised form 24 March 2015
Accepted 9 April 2015
Available online 11 April 2015

Keywords:
Hepatitis E virus
HEV
Genomic replicon
ORF-1
X-domain
Appr-1″-pase

ABSTRACT

The hepatitis E virus (HEV) ORF1 gene encodes the non-structural polyprotein wherein the 'X-domain' still remains poorly defined. Cellular X-domain associated macrodomain protein/ADP-ribose-1″-monophosphatase (Appr-1″-pase) activities are also reported in coronaviruses (CoV), including identification of its homologs in alpha and rubella viruses. The present study investigated the role(s) of X-domain residues in HEV replication cycle. In silico analysis showed a high degree of evolutionary conservation of X-domain (a.a. 785–942) a.a. positions wherein the N-terminus residues '*Asn806*, *Asn809*, *His812*, *Gly815*, *Gly816*, and *Gly817*' formed a potential catalytic-site homolog of CoVAppr-1″-pase. To experimentally test this prediction, X-domain 'active-site' residues were subjected to mutational analysis using the HEV-SAR55 replicon (*pSK-GFP*). FACS analysis of mutant RNA transfected S10-3 cells showed that *Gly816Ala* and *Gly817Ala* constructs completely abrogated HEV replication, similar to their *Gly816Val* and *Gly817Val* counterparts. However, '*Gly815Ala*' mutant replicated very poorly in contrast to '*Gly815Val*' that completely abolished GFP synthesis. Furthermore, while '*Asn806Ala*' mutant retained RNA replication, the '*Asn809Ala*' and *His812Leu* mutants showed non-viability. Notably, in a sequential-nucleotide mutation analysis, the dispensability of X-domain in HEV replication at transcriptional level has already been demonstrated (Parvez, 2013b). Taken together, the present data strongly argue for an essential role of X-domain residues (*Asn809*, *His812*, *Gly816* and *Gly817*) at post-translational level, indicating its involvement in viral replication. In conclusion, the speculated regulatory role of ORF1 X-domain in HEV replication cycle critically depends on the '*Asn*, *Asn*, *His*, *Gly*, *Gly*, *Gly*' segment/secondary structure. Nevertheless, further biochemical or biophysical characterizations of HEV X-domain associated Appr-1″-pase activity would only confirm its biological significance in virus or host-pathogenesis.

1. Introduction

Hepatitis E virus (HEV) is an emerging pathogen that causes acute hepatitis, in general (Aggarwal and Naik, 2009; Holla et al., 2013) as well as chronic liver disease in some individuals (Parvez, 2013a; Kamar et al., 2014). Classified as the only member of the *Hepeviridae* family, human HEV is recognized with at least four genotypes (HEV1, HEV2, HEV3, and HEV4). Compared to HEV1 and HEV2, HEV3 and HEV4 have potential zoonosis in swine, including some other mammalian species such as boar, deer, rat, rabbit, camel, and bat (Meng, 2013). The virus is non-enveloped with a plus-sense, single-stranded RNA genome (~7.2 kb) that contains three open reading frames: ORF1, ORF2 and ORF3 (Tam et al., 1991). Of these, ORF1 gene is the largest (5109 bases) that codes for the non-structural/replicase polyprotein of 1703 a.a. (~186 kDa), essential for viral replication cycle (Ansari et al., 2000; Parvez, 2013b). Based on amino acid (a.a.) sequence homology of plus-strand RNA virus polyproteins, Koonin et al. (1992) had proposed methyltransferase (MeT), papain-like cysteine protease (PCP), proline-rich (P), RNA helicase (Hel/NTPase) and RNA-dependent RNA polymerase (RdRp) as well as undefined 'X' and 'Y' domains within HEV ORF1.

The undefined domain 'X' belongs to the cellular ADP-ribose-1″-monophosphatase (Appr-1″-pase) of macrodomain protein family (Allen et al., 2003). The Appr-1″-pase is involved in the tRNA splicing pathway that catalyzes the conversion of ADP-ribose-1″-monophosphate (Appr-1″-p) to ADP-ribose (ADPR). So far, ~300 orthologs of X-domain have been identified in eukaryotes (Karras et al., 2005) as well as animal plus-strand RNA viruses like, coronaviruses (CoV), alphaviruses, rubella virus (RUBV) and HEV (Gorbalenya et al., 1991; Draker et al., 2006; Snijder et al., 2003; Ziebuhr, 2005). Among the CoV, X-domains of human CoV-229E (HCoV-229E), severe acute respiratory syndrome CoV (SARS-CoV), and porcine

Abbreviations: AA, Amino acid; Appr-1″-pase, ADP-ribose-1″-monophosphatase; Asn, Asparagine; CoV, Coronavirus; FACS, Fluorescence activated cell sorting; GFP, Green fluorescent protein; Gly, Glycine; HEV, Hepatitis E virus; His, Histidine; ORF, Open reading frame; PBS, Phosphate buffered saline; RNA, Ribonucleic acid; RUBV, Rubella virus; SARS-CoV, Severe acute respiratory syndrome CoV; TGEV, Transmissible gastroenteritis virus.

* Corresponding author.
E-mail address: khalid_parvez@yahoo.com.

http://dx.doi.org/10.1016/j.gene.2015.04.026
0378-1119/

transmissible gastroenteritis virus (TGEV) are shown to have an Appr-1″-pase activity, in vitro (Egloff et al., 2006; Putics et al., 2005; Saikatendu et al., 2005). Also, the structure of the SARS-CoV Nsp3 X-domain has been determined in isolation (Saikatendu et al., 2005) as well as in complex with ADPR (Egloff et al., 2006).

Though the X-domains have no significant sequence homology with phosphatases of known structure, few studies have revealed a common macrodomain fold, including four conserved stretches of a.a. residues that form the 'ADPR-binding' pocket/catalytic center (Kumaran et al., 2005; Shull et al., 2005; Karras et al., 2005; Egloff et al., 2006). Therein, the first stretch contains two *Asn* residues, of which the second *Asn* was reported essential for the Appr-1″-pase activity of HCoV-229E and SARS-CoV X-domains (Karras et al., 2005; Putics et al., 2005). Moreover, single a.a. substitutions within the alphavirus, Semliki Forest virus (SFV) X-domain have been shown to significantly suppress viral pathogenesis in infected mice (Tuittila and Hinkkanen, 2003). Therefore, viral X-domains are also proposed to interact with some cellular ADPR/macrodomain proteins, involved in host pathobiology (Karras et al., 2005). Conceivably, based on known sequence-function homology, the present study investigated the role(s) of X-domain conserved residues in HEV replication cycle, using the viral genomic-replicon/S10-3 culture model.

2. Material and methods

2.1. In silico analysis

GenBank database (NCBI) sequences ($n = 208$) of ORF1 X-domain (a.a. 785–942) of HEV strains representing the four genotypes, including genetically-related viruses and prokaryotic and eukaryotic sequences were analyzed, using *ClustalW 1.83* with a gap open penalty of −10 and gap extension penalty of −0.5 (http://embnet.vital-it.ch/software/ClustalW.html). The evolutionary conservation of HEV X-domain residue positions was predicted using *ConSurf* (http://bioinf.cs.ucl.ac.uk/psipred) that is based on the phylogenetic relations between homologous sequences (Glaser et al., 2003). The degree to which an a.a. position is evolutionarily conserved is strongly dependent on its structural and functional importance.

2.2. Construction of X-domain mutant-replicons

ORF1 X-domain a.a. mutants (*pSK-GFP-Asn806Ala*, *pSK-GFP-Asn809Ala*, *pSK-GFP-His812Leu*, *pSK-GFP-Gly815Ala*, *pSK-GFP-Gly816Ala* and *pSK-GFP-Gly817Ala*) were constructed in HEV1-SAR55 full-length (7.2 kb) genomic replicon (*pSK-GFP*) backbone (generous gift of Dr. Suzanne Emerson, National Institutes of Health, Bethesda, MD, USA) by site-directed mutagenesis as described previously (Parvez, 2013b). Briefly, two sets of mutant primers were designed and commercially synthesized (Invitrogen, USA). The polymerase chain-reaction (PCR) was carried out in a 50 μl reaction volume, using 10 ng of replicon DNA, appropriate amounts of primers, dNTP mix, DNA polymerase and polymerase buffer under thermal conditions as per the manufacturer's manual (TaKaRa Bio Inc., Japan). The amplicons (5.0 μl each) were verified by agarose gel electrophoresis to confirm the correct size of the plasmid. Further, each amplicon was digested with *Dpn I* (Invitrogen, USA) in a 10 μl reaction volume at 37 °C for 1.5 h. The digested mix (5 μl each) was transformed into DH5α XL-blue competent cells (Strata gene, USA) by the heat-shock method and plated on ampicillin-containing agar plates. Following an overnight incubation at 37 °C, bacterial colonies were picked and plasmids (Qiagen Plasmid Mini-prep Kit, Germany) were screened by restriction digestion. Mutant plasmids were confirmed by DNA sequencing (Invitrogen, USA) and stocks were prepared (Qiagen Plasmid Maxi-prep Kit, Germany).

2.3. Cell culture

Human hepatoma cell line, HuH7/S10-3 (generous gift of Dr. Suzanne Emerson, NIH, USA), was maintained in T75 culture flasks as described elsewhere (Emerson et al., 2004) at 37 °C with 5% CO_2 supply, and seeded in a 12-well (1.0×10^6 cells/well) or 24-well (0.5×10^6 cells/well) culture plate for further experiments.

2.4. In vitro transcription and transfection

The mutant replicons were transcribed in vitro in a 50 μl reaction volume, and capped-RNA mix was transfected into S10-3 cells essentially as described elsewhere (Emerson et al., 2004; Parvez et al., 2011). The yield and quality of all RNA samples were assessed by spectrophotometry (NanoDrop 2000, Thermo Scientific, USA) and agarose-gel electrophoresis prior to transfection. The transfected cells were incubated for 6 days at 34.5 °C, the preferred temperature to allow the RNA replication and production of GFP. S10-3 cultures transfected with wild-type transcript (*pSK-GFP-WT*) showing green fluorescence served as the positive control while those receiving replication of incompetent/defective transcript *pSK-GFP-G816V* or *pSK-GFP-G817V* (Parvez, 2013b) was included as the negative control. All transfections were done in duplicate and repeated.

2.5. Flow cytometry (FACS)

A 24-well culture plate (with duplicate samples) of transfected S10-3 cells was harvested on day 6 as described previously (Parvez et al., 2011). In sum, a culture well was treated with 100 μl trypsin (Invitrogen, USA) followed by adding 200 μl of 1× PBS. Wells were rinsed with another 200 μl of PBS and the cell suspensions were pooled (~500 μl/tube, final). The cells were pelleted at 4 °C, and re-suspended in 300 μl of cold PBS. The samples (in duplicate) in cold condition were immediately subjected to FACS scoring of GFP-positive cells (10,000 count/sample) and data (% gated events) analyzed.

3. Results

3.1. Conservation of X-domain 'Asn, Asn, His, Gly, Gly, Gly' position within HEV strains

Within the HEV X-domain sequences, *Asn806*, *Asn809*, *His812*, *Gly815*, *Gly816*, and *Gly817* residue positions were found highly conserved among human strains representing the recognized four viral genotypes (Fig. 1).

3.2. Identification of an evolutionary conserved putative ADPR-binding module

The *ConSurf* data revealed the conservation of HEV X-domain a.a., including the proposed Appr-1″-pase active-site residues (*Asn806*, *Asn809*, *His812*, *Gly815*, *Gly816*, and *Gly817*) when weighed against non-HEV orthologous sequences by the software (Fig. 2A). Notably, the purpose of this study was to characterize the putative active-site residues at molecular level. That's why these universally conserved six residues were analyzed excluding rest of the conserved sequences. Universally conserved positions of a.a. among members from the same protein family often reveal the importance of each position for the predicted protein's structure or function. Analysis of orthologous

Fig. 1. Multiple alignment ($n = 208$) analysis showing HEV ORF1 X-domain a.a. sequence conservation within the available HEV strains (NCBI GenBank), representing all four genotypes. The highly conserved '*Asn*/*N806*, *Asn*/*N809*, *His*/*H812*, *Gly*/*G815*, *Gly*/*G816* and *Gly*/*G817*' residues are indicated (red).

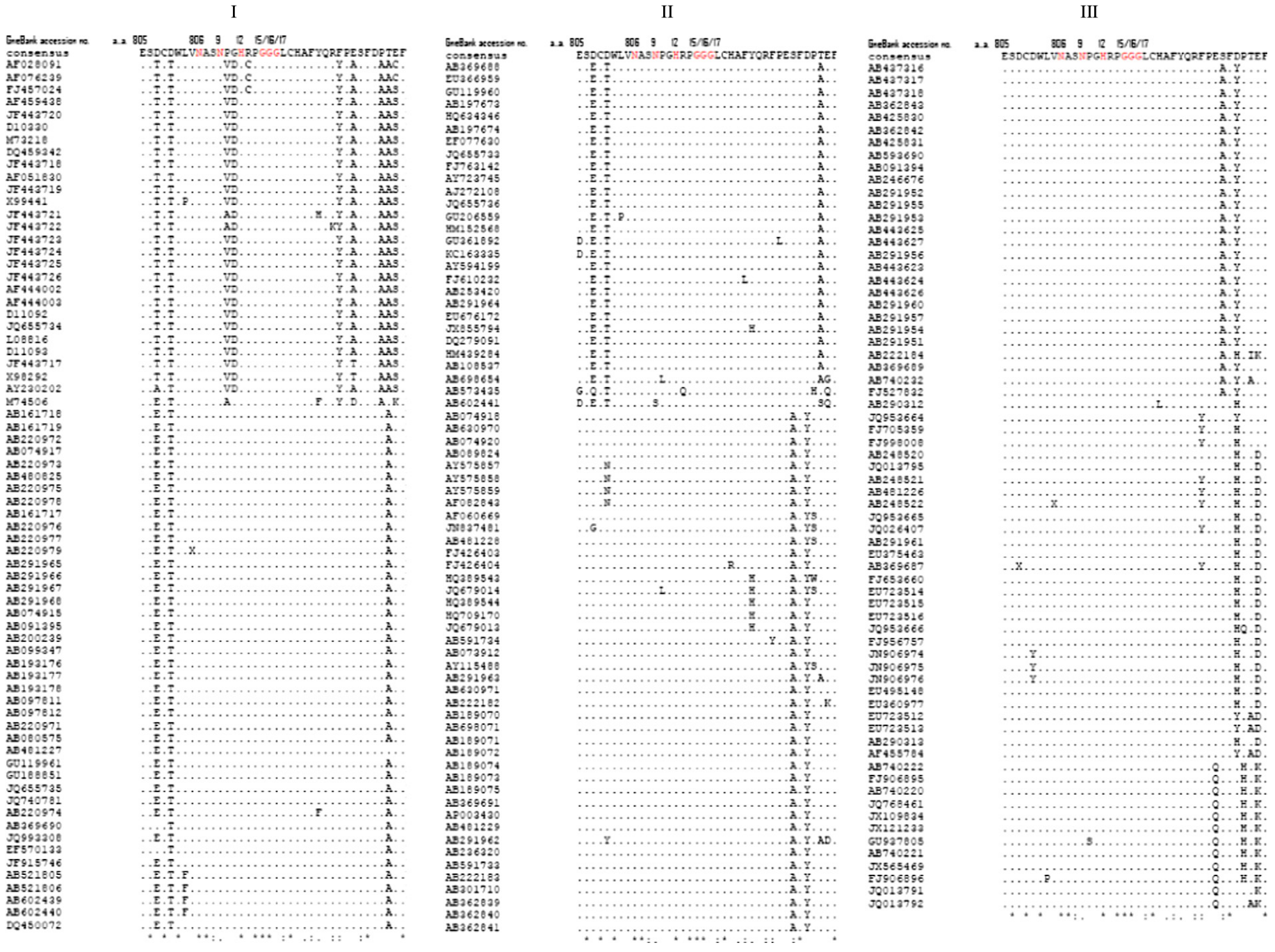
I
II
III
GneBank accession no.
a.a. 805 806 9 12 15/16/17
consensus ESDCDWLVNASNPGHRPGGGLCHAFYQRFPESFDPTEF

A

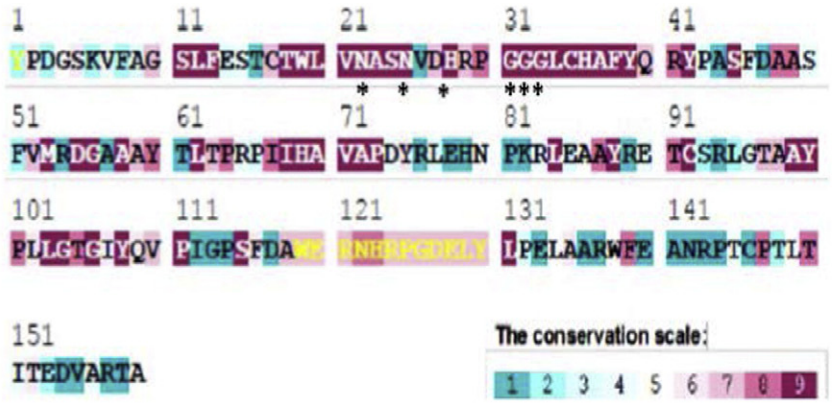

B

ID/Accession no.	Protein	Organism	Appr-1′-pase active-site
AF051830	Nonstructural X-domain	HEV	NASNVDHRPGGG
Q6X2S4	Nonstructural X-domain	RUBV	NASNVDHRPGGG
3ejg	Nonstructural X-domain	HCoV-229E	NANNENLAHGGG
2ACF	Nonstructural X-domain	SARS-CoV	NAANIH L KHGGG
R1AB_CVPPU	Nonstructural X-domain	TGEV	NAANGDLKHMGG
A0A069M8P	O-acetyl-ADP-ribose-deacetylase	S. enterica	NAANA S LMGGG
A0A084LB12	Uncharecterized protein	X. campestris	NAAN E S LLGGG
A0A077YQ63	ADP-ribose binding module	S. enterica I	NAAN A SLMGGG
A0A081BR51	Macro-H2A1-related protein	Bacterium UASB14	NAAN S S LLGGG
A0A087T7L1	Macrodomain containing protein 2	S. mimosarum	NAANNS L RGGG
A4J7T8	Appr-1-p processing domain protein	D. reducens	NAANT S L LGGG
F0B8W9	Macro H2A1-like phosphatase	X. vesicatoria	NAANE S LLGGG
G2DDQ3	RNase III inhibitor	R. pachyptila	NAANS S LL GGG
S4P8Y2	LRP16 protein	Specked wood butterfly	NAANS MLKGGG
V9KB20	DNA polymerase-catalytic subunit	Australian ghost shark	NAANKS LLGGG
3q6zA	PARP14-Macrodomain 1	H. sapiens	NASNEDLKHYGG
4iqyA	Proximal ADP-ribosyl-hydrolase MacroD2	H. sapiens	NASNA S LLGGG

Fig. 2. The evolutionary conservation of HEV X-domain residues weighed against non-HEV orthologous sequences. (A) *ConSurf* analysis showing the conservation of HEV X-domain a.a., including the proposed Appr-1″-pase active-site residues (indicated with asterisks). Numbering of a.a. is not in accordance with HEV1 sequences where residues *Asn806*, *Asn809*, *His812*, *Gly815*, *Gly816* and *Gly817* correspond to a.a. N22, N25, H28, G31, G32 and G33, respectively. (B) Summarized analysis of published macrodomain family/APPR-1″-pase protein active-sites of RNA viruses and prokaryote and eukaryote sequences (NCBI GenBank or Protein Data Bank). The data shows a tight sequence and positional homology of HEV X-domain '*Asn806*, *Asn809*, *His812*, *Gly815*, *Gly816*, and *Gly817*' residues with non-HEV counterparts.

sequences therefore identified the positional conservation of HEV X-domain '*Asn806*, *Asn809*, *His812*, *Gly815*, *Gly816*, *Gly817*' residues, a potential homolog of the published macrodomain/ADPR-binding protein/Appr-1″-pase active-sites of RNA viruses, prokaryotes and eukaryotes (Fig. 2B).

3.3. The X-domain evolutionary conserved residues are critical for RNA replication

The in silico predicted HEV X-domain associated Appr-1″-pase active-site residues were subjected to molecular analysis by introducing

Asn → Ala, *His → Leu* and *Gly → Ala* substitutions (Fig. 3A) in the replicon RNA. Mutational analysis did not grossly affect the mutant replicons because the RNA yield was similar to wild type in all cases (Fig. 3B). Notably, the '*Gly → Val*' mutants had been previously studied (Parvez, 2013b). Since differential phenotypic effect of '*Gly → Val*' compared to '*Gly → Ala*' had been observed on enzymatic activity in RUBV, the '*Gly → Ala*' mutants were compared with their '*Val*' counterparts. FACS analysis showed GFP-positive and negative cells in *pSK-GFP-WT* and *pSK-GFP-G816V* transfection controls, respectively (Fig. 4). Of the mutant replicons, *Gly816Ala* and *Gly817Ala* constructs completely abrogated HEV replication, similar to their *Gly816Val* and *Gly817Val* counterparts, respectively (Fig. 4). However, the *Gly815Ala* mutant replicated very poorly (~30%) in contrast to *Gly815Val* that rendered GFP synthesis similar to wild-type. Furthermore, upstream to '*Gly*' triad, while the *Asn806Ala* mutant retained RNA replication by approximately 65% compared to wild-type, *Asn809Ala* and *His812Leu* mutants showed non-viability (Fig. 4). This strongly suggested the essentiality of '*Asn809*, *His812*, *Gly816* and *Gly817*' residues in X-domain activity in virus replication that together with '*Asn806 and Gly815*' could potentially form the putative Appr-1″-pase active-site.

4. Discussion

Plus-strand RNA virus encoded X-domain associated Appr-1″-pase activity has been identified in HCoV-229E, SARS-CoV and TGEV, including its homologs in bovine transmissible virus (BoTV), RUBV, SFV, and HEV (Gorbalenya et al., 1991; Koonin et al., 1992; Putics et al., 2005; Draker et al., 2006). The predictions on potential active site residues derived from crystal structure as well as genetically-close viral X-domains, and available HEV sequence homology analysis led to map X-domain '*Asn806*, *Asn809*, *His812*, *Gly815*, *Gly816*, and *Gly817*' stretch that could constitute the HEV Appr-1″-pase active site. In the published X-domain crystal structures, the Appr-1″-pase active site includes a '*His*' followed by '*Gly-Gly-Gly*' residues and two upstream '*Asn*' residues. The '*Gly*' triad forms part of the loop that connects '*Asn*' containing β-strand 3 and α-helix 1. Similarly, in the ADPR-binding site of the CoV X-domains, the cleft is lined by the '*Gly*' triad at the C-terminus of the β3–α2 (L5) loop wherein the second *Gly* makes a bond with the distal ribose (Egloff et al., 2006).

This prediction (of putative HEV Appr-1″-pase active-site) was further tested experimentally using the *pSK-GFP* (viral full-length genomic replicon)/S10-3 culture system. In the present study, the replicon contained GFP reporter gene in place of HEV ORF2 coding sequences that could allow monitoring of viral RNA replication (Emerson et al., 2004). In our RNA transfections, ~50–60% cells show GFP-positivity with wild-type replicon compared to mock or *Gly816Val*/*Gly817Val* mutant-transfected GFP-negative cells (fluorescence microscopic observations). All a.a. mutant replicons were therefore, compared with controls for their replication fitness or viability by FACS scoring of GFP-positive/negative cells. In TGEV, papain-like protease 1($PL1^{pro}$) was shown to cleave the polyproteins (nsp2/nsp3) at *Gly879–Gly880* within the '*Gly878–Gly879–Gly880*' triad of the downstream X-domain that had an Appr-1″-pase activity, too (Putics et al., 2006). Likewise, downstream to its protease domain, RUBV polyprotein cleavage-substrate *Gly1300–Gly1301* within the X-domain '*Gly1299–Gly1300–Gly1301*' triad has been characterized (Chen et al., 1996). In line with this, I have previously demonstrated the indispensability of ORF1 X-domain *Gly816–Gly817* residues in the conserved '*Gly815–Gly816–Gly817*' triad in HEV replication that was however, predicted as viral PCP cleavage-substrate (Parvez, 2013b). This is supported by the yeast macrodomain protein crystal structure (Allen et al., 2003) suggesting the viral '*Gly*' triad's contribution in substrate-binding through main-chain atoms. Because the HEV X-domain *Gly → Val* (larger, branched side-chain) mutants had already been characterized (Parvez, 2013b), in the present study, the three '*Gly*' were substituted with small side-chain residue '*Ala*'. Thus, the three '*Gly → Ala*' mutant replicons were analyzed along with their '*Gly → Val*' counterparts to see their differential effects, if any, on HEV RNA replication. FACS analysis of transfected cells revealed that '*Gly816Ala* and *Gly817Ala*' completely abrogated RNA replication, similar to '*Gly816Val* and *Gly817Val*', respectively. However, '*Ala*' mutant of '*Gly815*' produced very little GFP, in contrast to its '*Val*' counterpart that completely abolished GFP synthesis. This was in absolute agreement with RUBV X-domain '*Gly1299–Gly1300–Gly1301*' triad where the second and third '*Gly*' when substituted to either '*Val*' or '*Ala*' produced non-viable replicons in cultured cells (Chen et al., 1996). In a biochemical study, Putics et al. (2005) showed that the '*Gly → Val*' substitutions reduced the CoV X-domain associated Appr-1″-pase activities more strongly than the corresponding '*Gly → Ala*' changes. Importantly, while the '*Gly*' triad is conserved in most CoVs,

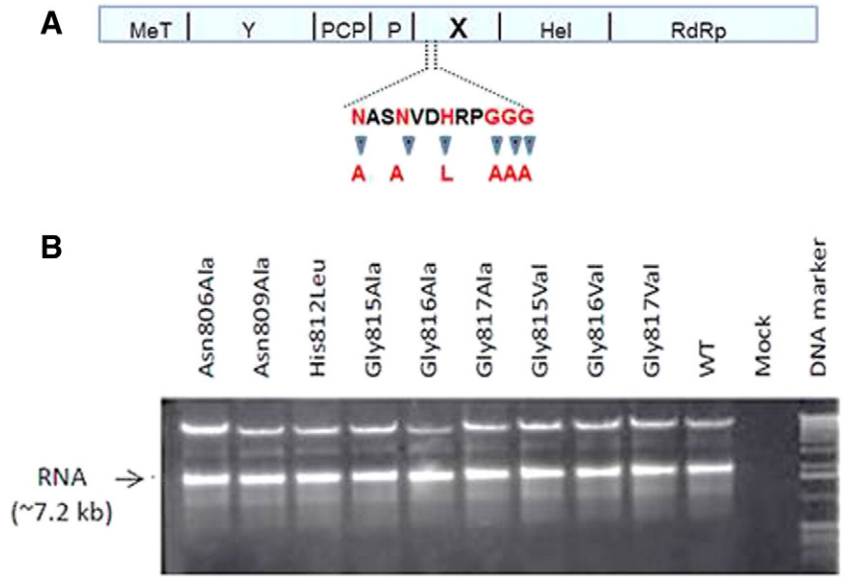

Fig. 3. Construction and synthesis of putative X-domain/Appr-1″-pase active-site a.a. mutants of HEV replicon. (A) Structural organization of HEV ORF1 gene, showing X-domain a.a. residue positions and substitutions (*Asn → Ala*, *His → Leu* and *Gly → Ala*). (B) A quantitative agarose-gel electrophoresis shows the in vitro synthesized replicon RNA constructs (5/50 μl RNA mix per well). The upper bands show the residual (untranslated) linear replicon DNA while the lower bands show the full-length viral RNA (indicated by arrow).

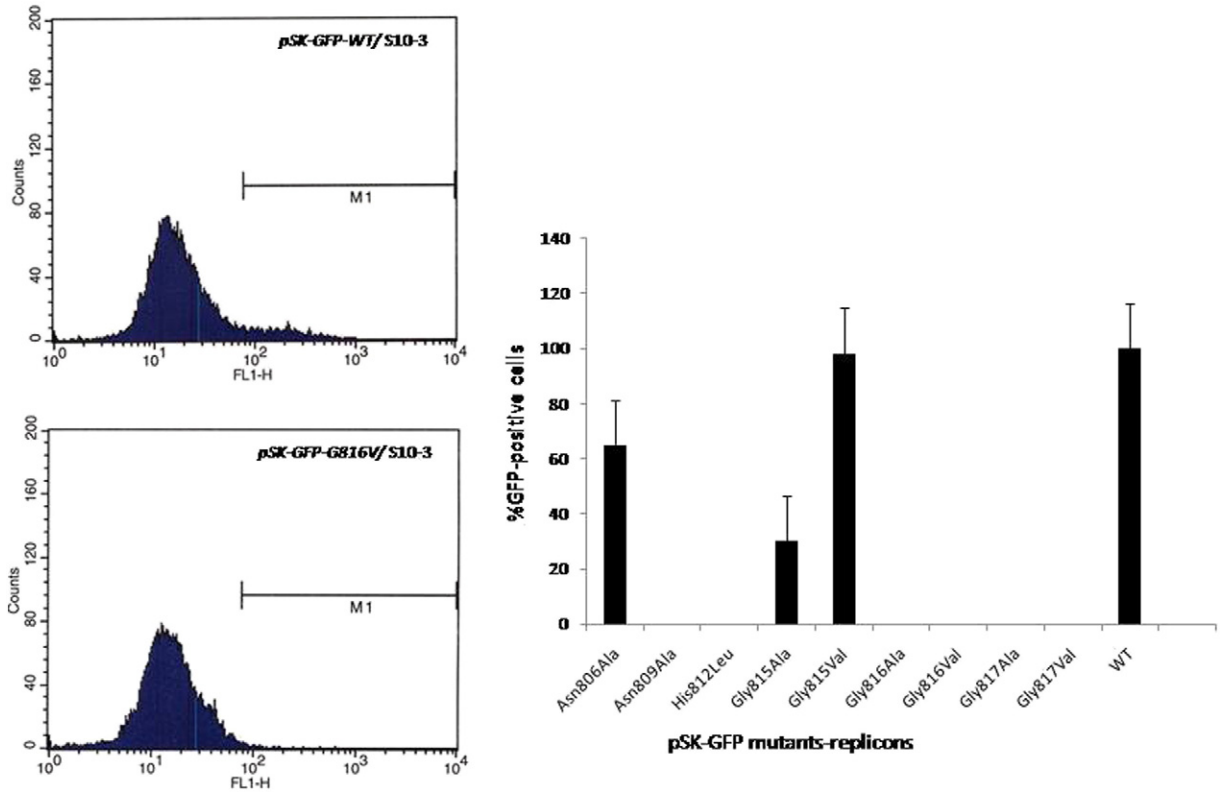

Fig. 4. FACS analysis of GFP expressions of mutant and wild-type replicon RNA-transfected S10-3 cells. The replication-fitness of *Gly → Val* (large and branched side-chain a.a.) mutant replicons is compared with *Gly → Ala* (small side-chain a.a.) counterparts. *pSK-GFP-WT* and *pSK-GFP-Gly816Val* served as the positive and negative controls, respectively.

the TGEV and feline CoV (FCoV) analogs have *Met* and *Val*, respectively at the first place (Fig. 1B), and substitution of the second or third '*Gly*' dramatically changes the X-domain structure. This strongly supports the essentiality of '*Gly816* and *Gly817*' residues in HEV X-domain activity and virus replication.

Furthermore, the homology data suggested that the HEV polyprotein X-domain residues '*Asn806*, *Asn809*, *His812*, *Gly815*, *Gly816*, and *Gly817*' corresponding to the HCoV-229E '*Asn1302*, *Asn1305*, *His1310*, *Gly111*, *Gly1312*, and *Gly1313*' form the putative active-site and might be involved in catalysis or substrate binding. In this study, while the HEV *Asn806Ala* mutant replicated to 2/3rd efficiency, *Asn809Ala* and *His812Leu* mutants completely abolished RNA replication. This was in conformity with HCoV-229E and SARS-CoV X-domain catalytic center residues where the second '*Asn*' was reported essential for Appr-1″-pase activity (Karras et al., 2005; Putics et al., 2005). Notably, in a sequential mutation analysis, the dispensability of X-domain nucleotides (nos. 2396–2910) in virus replication at transcriptional level has been clearly demonstrated (Parvez, 2013b). Taken together, the present data therefore, strongly argue for an essential role of X-domain a.a. residues (*Asn809*, *His812*, *Gly816*, and *Gly817*) at post-translational level, indicating its enzymatic (most likely, Appr-1″-pase) activity in HEV life cycle.

The X-domain's Appr-1″-pase activity or homologs are identified in animal RNA viruses but not in plant viruses. And interestingly, while the animal CoV, HCoV-229E X-domain was shown to bind ADP-ribose in vitro, its homolog of avian CoV, the infectious bronchitis virus (IBV) failed to do so despite structural similarity (Piotrowski et al., 2009). An explanation for this could be the host/substrate-specific activity of Appr-1″-pase that might provide a selective advantage in viral replication or/and modulation of host-factors during natural infection. In conclusion, the regulatory/catalytic role of ORF1 X-domain in HEV life cycle critically depends on '*Asn806*, *Asn809*, *His812*, *Gly815*, *Gly816*, *Gly817*' sequences/secondary structure elements that could be further modulated by the upstream PCP/P-domain. Nevertheless, biochemical or biophysical characterization of ORF1 X-domain associated Appr-1″-pase activity, including identification of relevant substrate(s) and their significance in virus or/and host remains inconclusive.

Acknowledgment

The author would like to extend his sincere appreciation to the Deanship of Scientific Research at King Saud University, Riyadh for its funding to this research through the research group project No. RG-1435-053.

References

Aggarwal, R., Naik, S., 2009. Epidemiology of hepatitis E: current status. J. Gastroenterol. Hepatol. 24, 1484–1493.
Allen, M.D., Buckle, A.M., Cordell, S.C., Lowe, J., Bycroft, M., 2003. The crystal structure of AF1521 a protein from *Archaeoglobus fulgidus* with homology to the non-histone domain of macroH2A. J. Mol. Biol. 330, 503–511.
Ansari, I.H., Nanda, S.K., Durgapal, H., Agrawal, S., Mohanty, S.K., Gupta, D., Jameel, S., Panda, S.K., 2000. Cloning, sequencing, and expression of the hepatitis E virus (HEV) nonstructural open reading frame 1 (ORF1). J. Med. Virol. 60, 275–283.
Chen, J.P., Strauss, J.H., Strauss, E.G., Frey, T.K., 1996. Characterization of the rubella virus non-structural protease domain and its cleavage site. J. Virol. 70, 4707–4713.
Draker, R., Roper, R.L., Petric, M., Tellier, R., 2006. The complete sequence of the bovine torovirus genome. Virus Res. 115, 56–68.
Egloff, M.P., Malet, H., Putics, A., et al., 2006. Structural and functional basis for ADP-ribose and poly(ADP-ribose) binding by viral macro domains. J. Virol. 80, 8493–8502.
Emerson, S.U., Nguyen, H., Graff, J., Stephany, D.A., Brockington, A., Purcell, R.H., 2004. In vitro replication of hepatitis E virus (HEV) genomes and of an HEV replicon expressing green fluorescent protein. J. Virol. 78, 4838–4846.
Glaser, F., Pupko, T., Paz, I., et al., 2003. ConSurf: identification of functional regions in proteins by surface-mapping of phylogenetic information. Bioinformatics 19, 163–164.
Gorbalenya, A.E., Koonin, E.V., Lai, M.M., 1991. Putative papain-related thiol proteases of positive-strand RNA viruses. Identification of rubi- and aphthovirus proteases and delineation of a novel conserved domain associated with proteases of rubi-, alpha- and coronaviruses. FEBS Lett. 288, 201–205.
Holla, R.P., Ahmad, I., Ahmad, Z., Jameel, S., 2013. Molecular virology of hepatitis E virus. Semin. Liver Dis. 33, 3–14.
Kamar, N., Dalton, H.R., Abravanel, F., Izopet, J., 2014. Hepatitis E virus infection. Clin. Microbiol. Rev. 27, 116–138.

Karras, G.I., Kustatscher, G., Buhecha, H.R., et al., 2005. The macro domain is an ADP-ribose binding module. EMBO J. 24, 1911–1920.
Koonin, E.V., Gorbalenya, A.E., Purdy, M.A., Rozanov, M.N., Reyes, G.R., Bradley, D.W., 1992. Computer-assisted assignment of functional domains in the nonstructural polyprotein of hepatitis E virus: delineation of an additional group of positive-strand RNA plant and animal viruses. Proc. Natl. Acad. Sci. U. S. A. 89, 8259–8263.
Kumaran, D., Eswaramoorthy, S., Studier, F.W., Swaminathan, S., 2005. Structure and mechanism of ADP-ribose-1-monophosphatase (Appr-1″ pase), a ubiquitous cellular processing enzyme. Protein Sci. 14, 719–726.
Meng, X.J., 2013. Zoonotic and foodborne transmission of hepatitis E virus. Semin. Liver Dis. 33, 41–49.
Parvez, M.K., 2013a. Chronic hepatitis E infection: risks and controls. Intervirology 56, 213–216.
Parvez, M.K., 2013b. Molecular characterization of hepatitis E virus ORF1 gene supports a papain-like cysteine protease (PCP)-domain activity. Virus Res. 178, 553–556.
Parvez, M.K., Purcell, R.H., Emerson, S.U., 2011. Hepatitis E virus ORF2 protein over-expressed by baculovirus in hepatoma cells, efficiently encapsidates and transmits the viral RNA to naïve cells. Virol. J. 8, 159–165.
Piotrowski, Y., Hansen, G., Boomaars-van der Zanden, A.L., et al., 2009. Crystal structures of the X-domains of a Group-1 and a Group-3 coronavirus reveal that ADP-ribose-binding may not be a conserved property. Protein Sci. 18, 6–16.
Putics, Á., Filipowicz, W., Hall, J., Gorbalenya, A.E., Ziebuhr, J., 2005. ADP-ribose-1″-monophosphatase: a conserved coronavirus enzyme that is dispensable for viral replication in tissue culture. J. Virol. 79, 12721–12731.
Putics, A., Gorbalenya, A.E., Ziebuhr, J., 2006. Identification of protease and ADP-ribose-1″-monophosphatase activities associated with transmissible gastroenteritis virus non-structural protein 3. J. Gen. Virol. 87, 651–656.
Saikatendu, K.S., Joseph, J.S., Subramanian, V., et al., 2005. Structural basis of severe acute respiratory syndrome coronavirus ADP-ribose-1″-phosphate dephosphorylation by a conserved domain of nsP3. Structure 13, 1665–1675.
Shull, N.P., Spinelli, S.L., Phizicky, E.M., 2005. A highly specific phosphatase that acts on ADP-ribose 1-phosphate, a metabolite of tRNA splicing in *Saccharomyces cerevisiae*. Nucleic Acids Res. 33, 650–660.
Snijder, E.J., Bredenbeek, P.J., Dobbe, J.C., et al., 2003. Unique and conserved features of genome and proteome of SARS-coronavirus, an early split-off from the coronavirus group 2 lineage. J. Mol. Biol. 331, 991–1004.
Tam, A.W., Smith, M.M., Guerra, M.E., Huang, C.C., Bradley, D.W., Fry, K.E., Reyes, G.R., 1991. Hepatitis E virus (HEV): molecular cloning and sequencing of the full-length viral genome. Virology 185, 120–131.
Tuittila, M., Hinkkanen, A.E., 2003. Amino acid mutations in the replicase protein nsP3 of Semliki Forest virus cumulatively affect neurovirulence. J. Gen. Virol. 84, 1525–1533.
Ziebuhr, J., 2005. The coronavirus replicase. Curr. Top. Microbiol. Immunol. 287, 57–94.